Superconducting magnetic shields for SQUID applications

J. R. Claycomb[a] and J. H. Miller, Jr.
Department of Physics and Texas Center for Superconductivity, University of Houston, Houston, Texas 77204-5932

(Received 25 May 1999; accepted for publication 1 September 1999)

We investigate the shielding of superconducting and μ-metal forms in axial and transverse directed background magnetic noise fields. Analytical expressions are obtained for the improvement in signal-to-noise ratio obtained by placing a superconducting disk in the presence of a dipole source and a uniform noise field. Axial and transverse shielding factors are then compared for identical superconducting and μ-metal cylinders. The signal-to-noise ratio is found to be infinite at certain points inside a superconducting cylinder as well as a superconducting cylinder with a central partition. Shielding factors obtained here are relevant to SQUID measurements of small dipole source fields in the presence of large background noise fields such as those encountered in biomagnetism and nondestructive evaluation. © *1999 American Institute of Physics.* [S0034-6748(99)03512-1]

I. INTRODUCTION

Superconducting quantum interference devices (SQUIDs) exhibit unsurpassed sensitivity to small changes in magnetic field. This ultrahigh field sensitivity makes SQUIDs ideal for low level magnetic measurements that would be impossible with conventional magnetometers. Unfortunately, the high magnetic field sensitivity of SQUIDs also inhibits their performance in the presence of electromagnetic noise sources such as the Earth's magnetic field and power-line signals. It is therefore necessary to eliminate these noise fields in order to measure small magnetic signals such as those encountered in biomagnetism and nondestructive evaluation.

The pickup of uniform noise signals from a SQUID can be reduced by measuring field gradients instead of the magnetic field directly. This typically involves the electronic subtraction of two SQUID outputs (for high-T_c SQUID applications), or the use of superconducting wire-wound gradiometers (for low-T_c SQUID applications). Alternatively, localized magnetic shielding can be used to selectively screen noise signals from the SQUID, allowing the detection of nearby dipole sources.

In this article, analytical solutions are developed for the magnetic field distribution inside superconducting and μ-metal shields having cylindrical symmetry. Shield geometries modeled here include superconducting and μ-metal cylinders, a superconducting disk, and a superconducting tube with a central superconducting partition. The field detected by a SQUID magnetometer is calculated for noise fields incident in axial and transverse directions with respect to the shields axis. The shielding factor and the improvement in signal-to-noise ratio is then obtained. In the case of a superconducting tube, nodal points are found where the signal-to-noise ratio becomes infinite.

[a]Electronic mail: Jclaycom@jetson.uh.edu

II. IMAGE SURFACE GRADIOMETRY

In electrostatics, the problem of an arbitrary charge distribution in the presence of a grounded conductor can be described in terms of an image charge distribution such that the electrostatic potential vanishes on the conducting surface. In magnetostatics, the image concept can be extended to simulate current sources in the presence of superconducting surfaces.[1] This concept has been employed in constructing superconducting image surface gradiometers[2,3] where a SQUID sensor positioned near a superconducting plate detects a source field proportional to its gradient dB_z/dz. Here, z is normal to both the SQUID pickup loop and the superconducting plate. In this case, the superconducting plate also serves to deflect distant uniform magnetic noise sources from the location of the SQUID.

The image gradiometry concept is illustrated in Fig. 1(a), where an infinite line current is located a distance L above a superconducting planar conductor. The field distribution in the region above the superconducting plane can be described as a superposition of the original current source and an image current flowing in the opposite direction a distance L beneath the superconducting surface. A magnetometer placed a height h above the superconducting plane will then detect the field produced by the source and screening currents in the superconductor. Here, the field produced by the screening currents is equivalent to the field produced by the image current. At point $P(x,h)$ in Fig. 1(a), the component of magnetic field detected by a SQUID (treated as a point magnetometer) whose sensing area is oriented normal to the superconducting plane is given by

$$B_z(P)=\frac{\mu_0 I}{2\pi}\left(\frac{x}{\sqrt{x^2+(z-h)^2}}-\frac{x}{\sqrt{x^2+(z+h)^2}}\right). \qquad (1)$$

Here, the superconducting plane is at $z=0$. If the superconducting plane is now removed [Fig. 1(b)], the magnetic field gradient at point P is approximately,

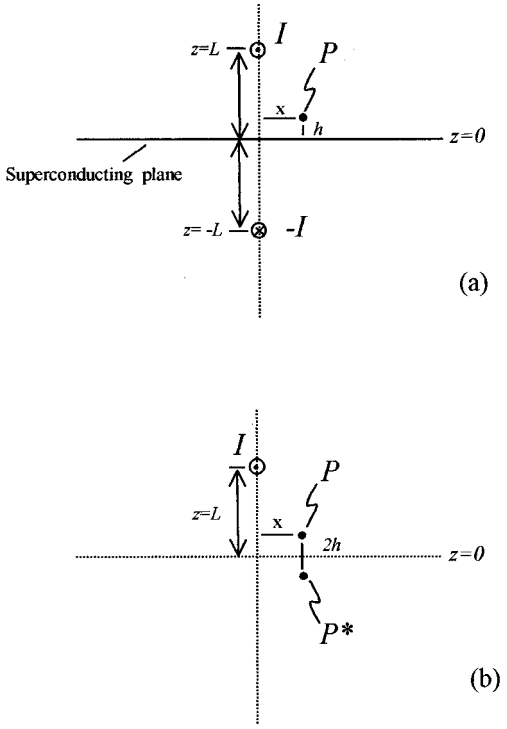

FIG. 1. Infinite wire carrying a current I (a) above an infinite superconducting plane and (b) in absence of the superconducting plane. Points P and P^* denote the location of point magnetometers measuring the z component of the magnetic field.

$$\frac{dB_z(P)}{dz} \simeq \frac{B_z(P) - B_z(P^*)}{2h}, \tag{2}$$

where P^* is at $(x,-h)$. This expression is the same as Eq. (1) divided by $2h$. The field detected by the magnetometer at point P with the shield present can then be expressed as

$$[B_z(P)]_{\text{w/shield}} = 2h\left[\frac{dB_z(P)}{dz}\right]_{\text{w.o./shield}}. \tag{3}$$

Hence, the SQUID output with the shield present is proportional to the field gradient without the shield present times twice the SQUID height above the shield. A SQUID positioned above a superconducting plane therefore acts as a first-order gradiometer with the disadvantage that the source field also vanishes as $h \to 0$.

In general, the signals of interest are produced by local current or magnetic dipole sources. We therefore compute the attenuation of several dipole sources for a given sensor position above the superconducting plane. The dipole attenuation is defined as the ratio of the shielded and unshielded values of the component of dipole field perpendicular to the SQUID pickup loop. For a dipole height L and SQUID height h above a superconducting plane, the attenuation Γ is given by

$$\Gamma(L,h) = \frac{[B_z]_{\text{w/shield}}}{[B_z]_{\text{w.o./shield}}} = 1 - \left(\frac{x^2 + (L-h)^2}{x^2 + (L+h)^2}\right)^{\alpha}, \tag{4}$$

where the z axis is perpendicular to the SQUID pickup loop. Substituting $\alpha = 1/2$ into expression (4) gives the attenuation of an infinite line source, while substituting $\alpha = 3/2$ gives the attenuation of current dipole displaced a distance x from the z axis. The current dipole, used extensively to model sources in biomagnetism and nondestructive testing, can be thought of as a current source and a current sink separated by a small distance. Substituting $\alpha = 3/2$ also gives the attenuation of a magnetic dipole, or a current loop of radius x, whose axis is normal to the superconducting plane. Here, $\Gamma = 1$ corresponds to zero attenuation, while $\Gamma = 0$ corresponds to a total attenuation of the dipole field. Clearly, the dipole signal vanishes in the limit of large dipole distance L, as well as small SQUID height h above the superconducting plane.

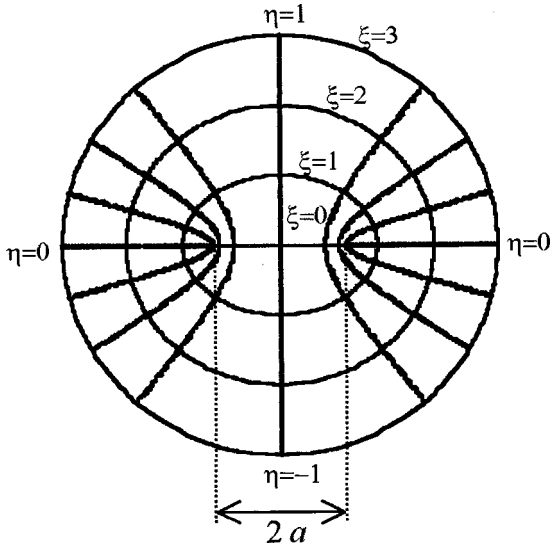

FIG. 2. Oblate spheroidal coordinate system. A thin superconducting disk of radius a is described by the surface $\xi = 0$. The positive z axis corresponds to the surface $\eta = 1$ and is measured from the center of the disk along the axis of symmetry.

III. SHIELDING OF A SUPERCONDUCTING DISK

In this section, the improvement in signal-to-noise ratio of a superconducting disk in the presence of a uniform noise field and a dipole source field is approximated. Here, we only consider the superconducting disk in an axial uniform noise field since, from symmetry, a SQUID centered above the disk will not pick up transverse field components.

The problem of a superconducting disk in an external magnetic field can be obtained by solving Laplace's equation for the magnetic scalar potential in oblate spheroidal coordinates. The analogous problem of an incompressible nonviscous fluid flow around a circular disk is treated by Morse and Feshbach.[4]

The oblate spheroidal coordinate system is shown in Fig. 2. The range of η is from -1 to $+1$. Surfaces of constant η are hyperboloids of one sheet. The surface $\eta = \pm 1$ corresponds to the $\pm z$ axis. The range of ξ is from 0 to ∞ and describes oblate spheroidal surfaces. The surface $\xi = 0$ corresponds to a disk located in the x-y plane of radius a, while the surface $\eta = 0$ corresponds to the remainder of the x-y plane excluding the disk. The azimuthal coordinate ϕ is the same as in cylindrical coordinates.

The magnetic field strength $H = B/\mu$ is expressed as the gradient of a scalar function Ω,

$$\mathbf{H} = -\nabla\Omega. \tag{5}$$

Since $\nabla \cdot \mathbf{H}=0$, Ω satisfies Laplace's equation $\nabla^2\Omega=0$ which is written as

$$\frac{1}{a(\xi^2+\eta^2)}\left[\frac{\partial}{\partial\xi}(\xi^2+1)\frac{\partial\Omega}{\partial\xi}+\frac{\partial}{\partial\eta}(1-\eta^2)\frac{\partial\Omega}{\partial\eta}+\frac{(\xi^2+\eta^2)}{(\xi^2+1)(1-\eta^2)}\frac{\partial^2\Omega}{\partial\phi^2}\right]=0. \tag{6}$$

This equation is solved by the method of separation of variables. Substituting $\Omega=\Xi(\xi)Z(\eta)\Phi(\phi)$ into Eq. (6) gives separated functions of the form

$$\Xi(\xi)Z(\eta)\Phi(\phi)=\begin{Bmatrix}P_n^m(i\xi)\\Q_n^m(i\xi)\end{Bmatrix}\begin{Bmatrix}P_n^m(\eta)\\Q_n^m(\eta)\end{Bmatrix}\begin{Bmatrix}e^{im\phi}\\e^{-im\phi}\end{Bmatrix}, \tag{7}$$

where P_n^m and Q_n^m are Legendre functions of the first and second kind. In general, the $P_n^m(i\xi)$ and $Q_n^m(\eta)$ diverge as $\xi\to\infty$ and $\eta\to1$, respectively. We therefore choose the $P_n^m(\eta)$ and the $Q_n^m(i\xi)$ in constructing a general solution to Ω. The scalar potential corresponding to a uniform field in the z direction is given by

$$\Omega=-H_0a\xi\eta, \tag{8}$$

where $z=a\xi\eta$. The potential form satisfying the boundary condition at infinity is then

$$\Omega=\sum_n A_nQ_n(i\xi)P_n(\eta)-H_0a\xi\eta. \tag{9}$$

The A_n are now found so that the normal field component vanishes on the superconducting disk. Here, we require that $\partial\Omega/\partial\xi=0$ when $\xi=\xi_0$ which gives

$$\sum_n A_nQ_n'(i\xi)P_n(\eta)=H_0a\eta. \tag{10}$$

Since $P_1(\eta)=\eta$ only the $n=1$ term survives so that

$$A_1=\frac{H_0a}{Q_1'(i\xi_0)}. \tag{11}$$

For a thin superconducting disk, we take $\xi_0=0$ so that the scalar potential now becomes

$$\Omega=H_0a\eta\left(\frac{2}{\pi}Q_1(i\xi)-\xi\right), \tag{12}$$

where $Q_1(i\xi)=\xi\cot^{-1}\xi-1$. It turns out that a transverse magnetic field relative to the shield axis is unattenuated by the disk, while an axial field $H_0\hat{z}$ falls off as

$$H_z=H_0\left[1-\frac{2}{\pi}\left(\tan^{-1}\frac{a}{z}-\frac{az}{a^2+z^2}\right)\right]. \tag{13}$$

Here, z coincides with the axis of the disk, which is located at $z=0$. For $z\ll a$, Eq. (13) becomes

$$H_z\approx H_0\frac{4}{\pi}\frac{z}{a}. \tag{14}$$

This corresponds to a shielding factor of $\pi a/4h$ for a point magnetometer located a distance h above the disk. The signal-to-noise improvement ratio (SNIR), defined as the shielding factor times the attenuation of a dipole source field, can then be approximated as

$$\mathrm{SNIR}\approx\frac{\pi a}{4h}\Gamma(L,h), \tag{15}$$

where $\Gamma(L,h)$ is given by Eq. (4). The SNIR can also be defined as the gain in SNR due to the shield, or the ratio of SNR values with and without the shield.

As a numerical example, the shielding factor 1 mm above a superconducting disk of radius 5 cm is 39.3. For an on-axis magnetic dipole with $L=2.5$ cm and $h=1$ mm, the attenuation $\Gamma(L,h)=0.21$. The SNIR is then computed as $0.21\times39.3=8.25$. This value is compared to a numerical finite element method (FEM) calculation[5] which gives an SNIR=7.07. For a magnetic dipole located 1.0 cm above the disk, the SNIR from Eq. (15) is 17.76 (compared to the FEM value of 14.84). Here, deviations from the FEM values result from the infinite plane approximation in calculating Γ for a finite size disk. A more exact calculation of SNIR will involve the expansion of the dipole source field in oblate spheroidal harmonics and solving the corresponding boundary value problem.

IV. SHIELDING PROPERTIES OF A SEMI-INFINITE SUPERCONDUCTING TUBE

A. Shielding of axial fields

Analytical expressions for the field distribution, as well as the attenuation of axial and transverse magnetic fields, inside a semi-infinite superconducting tube can be obtained from the scalar magnetic potential in cylindrical coordinates.[6] In this work, expressions are derived for the ''nodal points'' inside the tube where certain field components vanish identically. A complete description of the field inside the tube can also be obtained providing one of the field components is known in the opening of the tube.

The geometry of the tube is shown in Fig. 3. In order to obtain the field distribution inside the tube, we must first solve for Ω as before. Application of the scalar Laplacian in cylindrical coordinates gives

$$\frac{1}{\rho}\frac{\partial}{\partial\rho}\left(\rho\frac{\partial\Omega}{\partial\rho}\right)+\frac{1}{\rho^2}\frac{\partial^2\Omega}{\partial\phi^2}+\frac{\partial^2\Omega}{\partial z^2}=0. \tag{16}$$

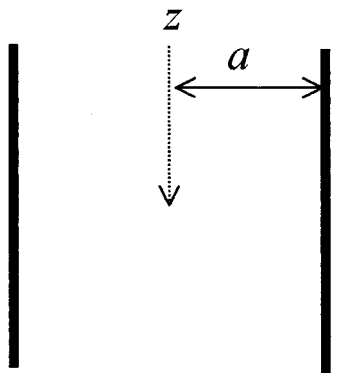

FIG. 3. Semi-infinite superconducting tube of radius a. The axis of symmetry corresponds to the z axis which is measured from the mouth of the tube inward.

By substituting $\Omega = R(r)\Phi(\phi)Z(z)$ into Eq. (16), a general solution is obtained as a product of functions of the form

$$R(\rho)\Phi(\phi)Z(z) = \begin{Bmatrix} J_m(k_m\rho) \\ N(k_m\rho) \end{Bmatrix} \begin{Bmatrix} e^{im\phi} \\ e^{-im\phi} \end{Bmatrix} \begin{Bmatrix} e^{+k_m z} \\ e^{-k_m z} \end{Bmatrix}. \tag{17}$$

The Bessel functions $J_m(k_m\rho)$ are chosen so that the potential is finite at the origin. The general solution of the scalar potential then becomes

$$\Omega(\rho,\phi,z) = \sum_{m=0}^{\infty} \sum_{n=1}^{\infty} J_m(k_{mn}\rho)\exp(\pm k_{mn}z) \times (A_{mn}\cos m\phi + B_{mn}\sin m\phi). \tag{18}$$

The field components are then given by

$$\begin{pmatrix} H_\rho \\ H_\phi \\ H_z \end{pmatrix} = -\begin{pmatrix} \dfrac{\partial\Omega}{\partial\rho} \\ \dfrac{1}{\rho}\dfrac{\partial\Omega}{\partial\phi} \\ \dfrac{\partial\Omega}{\partial z} \end{pmatrix}. \tag{19}$$

If the magnetic field is parallel to the axis of the cylinder, there is no ϕ dependence and only the $m=0$ term remains. For points inside the tube where $z>0$, only the negative exponential satisfies the boundary condition at $z=\infty$ so that Eq. (18) simplifies to

$$\Omega(\rho,z) = \sum_{n=1}^{\infty} A_{0n}J_0(k_{0n}\rho)\exp(-k_{0n}z). \tag{20}$$

The appropriate boundary condition on the inside tube wall is that $\hat{n}\cdot\mathbf{H}=0$ or $H_\rho=0$. This boundary condition is enforced by requiring that $(\partial/\partial\rho)J_0(k_{0n}\rho)=0$ at $\rho=a$ so that the components of the magnetic field become

$$H_\rho = -\sum_{n=1}^{\infty} A_{0,n}\frac{k'_{0,n}}{a}J'_0\left(k'_{0,n}\frac{\rho}{a}\right)\exp\left(-k'_{0,n}\frac{z}{a}\right), \tag{21}$$

$$H_z = \sum_{n=1}^{\infty} A_{0,n}\frac{k'_{0,n}}{a}J_0\left(k'_{0,n}\frac{\rho}{a}\right)\exp\left(-k'_{0,n}\frac{z}{a}\right), \tag{22}$$

where $k'_{0,n}$ are the roots of $J'_0(x)=0$. The slowest mode of decay is given by the first root of $J'_0(x)=0$ or $k'_{01}=3.832$ so that the field is attenuated along the tube axis at least as fast as

$$H_{\text{axial}} \propto \exp\left(-3.832\frac{z}{a}\right). \tag{23}$$

The values of $A_{0,n}$ can be obtained from knowledge of one of the field components at $z=0$. In general, the field distribution in the tube opening is not known but may be obtained from a numerical solution. Assuming that H_z is known at $z=0$,

$$H_z(\rho,z=0) = \sum_{n=1}^{\infty} A_{0,n}\frac{k'_{0,n}}{a}J_0\left(k'_{0,n}\frac{\rho}{a}\right). \tag{24}$$

Multiplying both sides of this expression by $\rho J_0[k'_{0,n}(\rho/a)]$ and integrating over the tube radius gives

$$\int_0^a \rho J_0\left(k'_{0,n'}\frac{\rho}{a}\right)H_z(\rho,0)d\rho = \sum_{n=1}^{\infty} A_{0,n}\frac{k'_{0,n}}{a}\int_0^a \rho J_0\left(k'_{0,n}\frac{\rho}{a}\right) \times J_0\left(k'_{0,n'}\frac{\rho}{a}\right)d\rho. \tag{25}$$

Making use of the identity

$$\int_0^a \rho J_m\left(k'_{m,n}\frac{\rho}{a}\right)J_m\left(k'_{m,n'}\frac{\rho}{a}\right)d\rho = \frac{a^2}{2}\left(1-\frac{m^2}{k'^2_{m,n}}\right)J_m^2(k'_{m,n})\delta_{n,n'}, \tag{26}$$

and solving for the $A_{0,n}$ gives

$$A_{0,n} = \frac{2}{ak'_{0,n}J_0^2(k'_{0,n})}\int_0^a \rho J'_0\left(k'_{0,n}\frac{\rho}{a}\right)H_z(\rho,0)d\rho. \tag{27}$$

The field components are now written as

$$H_\rho = -\sum_{n=1}^{\infty}\frac{2}{a^2}\frac{J'_0\left(k'_{0,n}\frac{\rho}{a}\right)}{J_0^2(k'_{0,n})}\exp\left(-k'_{0,n}\frac{z}{a}\right) \times \int_0^a \rho J_0\left(k'_{0,n}\frac{\rho}{a}\right)H_z(\rho,0)d\rho, \tag{28}$$

$$H_z = \sum_{n=1}^{\infty}\frac{2}{a^2}\frac{J_0\left(k'_{0,n}\frac{\rho}{a}\right)}{J_0^2(k'_{0,n})}\exp\left(-k'_{0,n}\frac{z}{a}\right) \times \int_0^a \rho J'_0\left(k_{0,n}\frac{\rho}{a}\right)H_z(\rho,0)d\rho. \tag{29}$$

From Eq. (29) we find that for a given mode, there is at least one point along the tube radius where $J_0[k'_{0,n}(\rho/a)]$ and hence H_z vanishes. These nodal points form a ring of radius

$$\rho_c = a\frac{k_{0,n}}{k'_{0,n}}, \tag{30}$$

where $k_{0,n}$ are the roots of $J_0(x)=0$. Deep inside the tube, where the contribution from higher order modes is negligible, ρ_c has a limiting value of $0.628a$, where a is the tube radius. The value of ρ_c agrees with FEM calculations.[5] The highest degree of magnetic shielding from axial noise fields is then obtained by positioning a SQUID with its pickup loop axis parallel to the shield axis at ρ_c. A caveat here is that transversely directed fields will contribute to a nonzero H_z at this location. The planar symmetry of a tube of finite length can then be exploited to overcome this problem.

B. Shielding of transverse magnetic fields

We now consider the case of an x-directed magnetic field transverse to the superconducting tube axis. The unshielded magnetic field is of the form

$$\mathbf{H} = H_0\hat{x} = H_0(\hat{\rho}\cos\phi - \hat{\phi}\sin\phi). \tag{31}$$

In the absence of the tube, the corresponding scalar potential is

$$\Omega = H_0 \rho \cos\phi. \tag{32}$$

The general solution to Ω now becomes

$$\Omega(\rho,\phi,z) = \sum_{m=1,3,5,\ldots}^{\infty} \sum_{n=1}^{\infty} A_{m,n} J_m\left(k'_{m,n}\frac{\rho}{a}\right) \exp\left(-k'_{m,n}\frac{z}{a}\right) \times \cos m\phi. \tag{33}$$

From symmetry only the odd order Bessel functions contribute to a nonzero radial magnetic field along the shield axis, hence the sum is taken only over odd values of m. The three components of magnetic field are then given by

$$H_\rho = -\sum_{m=1,3,5,\ldots}^{\infty} \sum_{n=1}^{\infty} A_{m,n} \frac{k'_{m,n}}{a} J'_m\left(k'_{m,n}\frac{\rho}{a}\right) \exp\left(-k'_{m,n}\frac{z}{a}\right) \times \cos m\phi, \tag{34}$$

$$H_\phi = \sum_{m=1,3,5,\ldots}^{\infty} \sum_{n=1}^{\infty} A_{m,n} \frac{m}{\rho} J_m\left(k'_{m,n}\frac{\rho}{a}\right) \exp\left(-k'_{m,n}\frac{z}{a}\right) \times \sin m\phi, \tag{35}$$

$$H_z = \sum_{m=1,3,5,\ldots}^{\infty} \sum_{n=1}^{\infty} A_{m,n} \frac{k'_{m,n}}{a} J_m\left(k'_{m,n}\frac{\rho}{a}\right) \exp\left(-k'_{m,n}\frac{z}{a}\right) \times \cos m\phi. \tag{36}$$

Here, the mode with the slowest fall off corresponds to $k'_{1,1}$ or the first root of $J'_1(x)=0$, so that the transverse field will fall off as fast as

$$H_{\text{trans}} \propto \exp\left(-1.84\frac{z}{a}\right). \tag{37}$$

As before the $A_{m,n}$ are evaluated with a prior knowledge of one of the field components in the tube opening. We note that for an x-directed applied field both H_z and H_ρ vanish in the plane $\phi=\pm\pi/2$, while H_ϕ vanishes in the plane $\phi=0,\pi$. In this case, both H_z and H_ϕ also vanish along the z axis. For an arbitrarily directed field consisting of both transverse and axial components, H_z vanishes at the intersection of the plane $\phi=\pm\pi/2$ and the surface of revolution $\rho_c = a \cdot k_{0,n}/k'_{0,n}$. SQUIDs positioned at these locations will not pick up any signal due to a uniform noise field having both an x and a z component.

In general, transverse noise fields can have both an x and a y component so that it may not be possible to position SQUIDs in a region of exactly zero H_z. This problem is solved if one considers a superconducting tube of finite length. From symmetry it is evident that there will be no axial field component due to an x- or a y-directed field in the central plane of the tube. The results of a FEM calculation are shown in Fig. 4 where the flux lines of a transverse applied noise field flatten out in the center of the tube. Since no flux lines cross the central plane (denoted by the dotted line), a SQUID positioned there will have a null output. The SQUID can then be positioned at the corresponding nodal point along the tube radius for rejection of the axial field component as well.

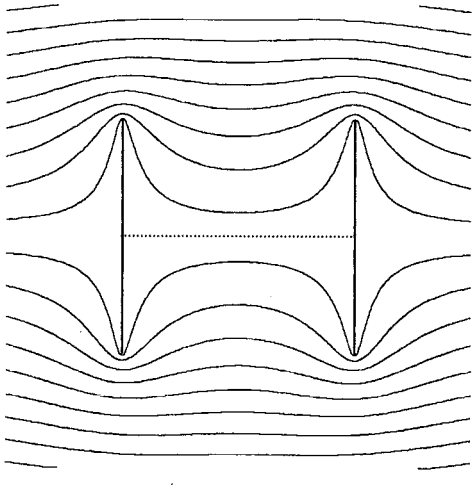

FIG. 4. Flux lines inside a superconducting tube of finite length due to a transverse applied magnetic field. Notice that flux lines do not cross the central plane denoted by the dotted line.

As a special case of a finite length superconducting tube, we consider a flat superconducting ring. From symmetry SQUIDs positioned in the opening of the ring will not pick up transverse fields. SQUIDs located at the nodal points in the ring will also reject axial noise fields. The flux lines produced by a local dipole source, on the other hand, will penetrate the nodal points in the ring and are detected by the SQUID. The SQUID system noise level is then determined by intrinsic sensor noise, system electronics, and noise due to flux motion (or vortex hopping) in the bulk of the shield.

V. SHIELDING PROPERTIES OF A SEMI-INFINITE μ-METAL TUBE

Expressions for the field distribution inside a semi-infinite μ-metal tube are derived in this section. The geometry of the tube is the same as the superconducting tube in Fig. 3. We show that the attenuation of a transverse field by a μ-metal cylinder is the same as the attenuation of an axial field along the axis of a superconducting tube.

For an ideal μ-metal shield, the value of μ_r is taken to be infinite ($\mu_r=0$ for a superconductor). The appropriate boundary condition on the tube wall is that the tangential component of H vanish. This boundary condition is enforced by requiring that $H_z=0$ or $J_0(k_{0n}\rho)=0$ at $\rho=a$. If the shield is placed in a region of uniform magnetic induction along the z axis, the field components inside the shield are given by

$$H_\rho = -\sum_{n=1}^{\infty} A_{0,n} \frac{k_{0,n}}{a} J'_0\left(k_{0,n}\frac{\rho}{a}\right) \exp\left(-k_{0,n}\frac{z}{a}\right), \tag{38}$$

$$H_z = \sum_{n=1}^{\infty} A_{0,n} \frac{k_{0,n}}{a} J_0\left(k_{0,n}\frac{\rho}{a}\right) \exp\left(-k_{0,n}\frac{z}{a}\right). \tag{39}$$

The $k_{0,n}$ corresponds to the roots of $J_0(x)=0$. The smallest root here is 2.405 so that the axial field decays as

$$H_{\text{axial}} \propto \exp\left(-2.405\frac{z}{a}\right), \tag{40}$$

which falls off slower than the axial field inside the superconducting tube. FEM calculations show that the free space field value actually increases near the opening of the μ-metal tube.

The field components inside the μ-metal tube due to an x-directed, transverse uniform field are given by

$$H_\rho = -\sum_{m=1,3,5,\ldots}^{\infty}\sum_{n=1}^{\infty} A_{m,n}\frac{k_{m,n}}{a}J'_m\left(k_{m,n}\frac{\rho}{a}\right)\exp\left(-k_{m,n}\frac{z}{a}\right) \times \cos m\phi, \tag{41}$$

$$H_\phi = \sum_{m=1,3,5,\ldots}^{\infty}\sum_{n=1}^{\infty} A_{m,n}\frac{m}{\rho}J_m\left(k_{m,n}\frac{\rho}{a}\right)\exp\left(-k_{m,n}\frac{z}{a}\right) \times \sin m\phi, \tag{42}$$

$$H_z = \sum_{m=1,3,5,\ldots}^{\infty}\sum_{n=1}^{\infty} A_{m,n}\frac{k_{m,n}}{a}J_m\left(k_{m,n}\frac{\rho}{a}\right)\exp\left(-k_{m,n}\frac{z}{a}\right) \times \cos m\phi. \tag{43}$$

Here, the smallest root corresponds to $k_{1,1}=3.834$ so that transverse field decays as

$$H_{\text{trans}} \propto \exp\left(-3.834\frac{z}{a}\right). \tag{44}$$

The transverse shielding of a μ-metal tube is therefore larger than that of a superconducting tube with the same radius. Equation (44) is also the same as the expression for the attenuation of an axial field inside a superconducting tube. This suggests that combinations of μ-metal and superconducting shielding may be used for reduction of both axial and transverse noise field components.

VI. SUPERCONDUCTING TUBE WITH A CENTRAL PARTITION

A superconducting tube with a central partition, or the ''H-shaped'' cylinder, was originally proposed as a noise shield for magnetocardiography in our lab.[7] Here, the shield consists of a superconducting tube of radius a joined with a superconducting disk at the center of the tube. The corresponding cross section of the shield has an H shape as shown in Fig. 5.

The same boundary conditions apply to the walls of the superconducting tube as before, only now we require that H_z vanishes on the superconducting disk. For a uniform field incident along the z axis, the field components inside the shield are given by

$$H_\rho = \mp\sum_{n=1}^{\infty} A_{0,n}\frac{k'_{0,n}}{a}J'_0\left(k'_{0,n}\frac{\rho}{a}\right)\cosh\left(k'_{0,n}\frac{z}{a}\right), \tag{45}$$

$$H_z = \pm\sum_{n=1}^{\infty} A_{0,n}\frac{k'_{0,n}}{a}J_0\left(k'_{0,n}\frac{\rho}{a}\right)\sinh\left(k'_{0,n}\frac{z}{a}\right). \tag{46}$$

Here, the upper and lower sign designate the upper and lower halves of the H-cylinder, respectively. For an H-shaped cylinder of height h, the range of z is between $-h/2$ and $+h/2$ with the superconducting disk at $z=0$. A superconducting tube with an end cap can also be modeled by taking the upper sign and a range of z between 0 to $+h/2$. In both cases, the attenuation along the z axis is given by

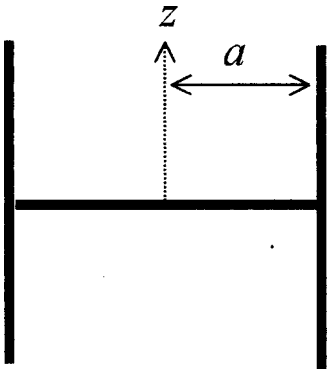

FIG. 5. Superconducting tube of radius a with a central disk shaped partition. The axis of symmetry corresponds to the z axis which is measured from the center of the disk.

$$H_{\text{axial}} \approx \sinh\left(3.834\frac{z}{a}\right). \tag{47}$$

As in the case of a hollow superconducting tube, nodal points can be found where $H_z=0$. For an x-directed uniform field, the field components inside the shield are written as

$$H_\phi = \sum_{m=1,3,5,\ldots}^{\infty}\sum_{n=1}^{\infty} A_{m,n}\frac{m}{\rho}J_m\left(k_{m,n}\frac{\rho}{a}\right)\cosh\left(k_{m,n}\frac{z}{a}\right)\sin m\phi, \tag{48}$$

$$H_z = \sum_{m=1,3,5,\ldots}^{\infty}\sum_{n=1}^{\infty} A_{m,n}\frac{k_{m,n}}{a}J_m\left(k_{m,n}\frac{\rho}{a}\right)\sinh\left(k_{m,n}\frac{z}{a}\right) \times \cos m\phi, \tag{49}$$

$$H_\rho = -\sum_{m=1,3,5,\ldots}^{\infty}\sum_{n=1}^{\infty} A_{m,n}\frac{k_{m,n}}{a}J'_m\left(k_{m,n}\frac{\rho}{a}\right)\cosh\left(k_{m,n}\frac{z}{a}\right) \times \cos m\phi. \tag{50}$$

The transverse field attenuation along the z axis is then given by

$$H_{\text{trans}} \approx \cosh\left(1.84\frac{z}{a}\right). \tag{51}$$

Expressions (48)–(50) are also valid for a hollow superconducting tube of height h without the superconducting partition. From Eq. (49) we see that H_z vanishes in the central plane $z=0$ of a hollow superconducting tube of finite length as previously argued from symmetry.

VII. DISCUSSION

Some of the key results of the previous sections are listed in Table I. In summary, the axial shielding factor of a superconducting tube is greater than the axial shielding factor of a μ-metal tube. It turns out that the axial shielding factor of a superconducting tube is the same as the transverse shielding factor of an identical μ-metal tube along the shield

TABLE I. Attenuation along the axis of several shielding geometries.

Shield type	Attenuation of H_{axial}	Attenuation of H_{trans}
Superconducting disk	$\frac{4}{\pi}\frac{z}{a}$ $(z \ll a)$	0
Superconducting tube	$\exp\left(-3.834\frac{z}{a}\right)$	$\exp\left(-1.84\frac{z}{a}\right)$
μ-metal tube	$\exp\left(-2.405\frac{z}{a}\right)$	$\exp\left(-3.834\frac{z}{a}\right)$
Superconducting H-shape tube	$\sinh\left(3.834\frac{z}{a}\right)$	$\cosh\left(1.84\frac{z}{a}\right)$

axis. The transverse shielding factor of a μ-metal tube is also greater than the transverse shielding factor of a superconducting tube. These results suggest that combinations of superconducting and μ-metal shields may serve to effectively screen both transverse and axial noise field components.

Figure-of-merit calculations were also made for a superconducting disk in oblate spheroidal coordinates including the shielding factor and the SNIR. Here, approximate expressions were obtained for the SNIR with both current and magnetic dipole sources.

Finally, expressions were obtained for the nodal points inside a semi-infinite superconducting tube where the axial noise field component vanishes entirely. For a finite length superconducting tube, it was shown that there is no pickup due to a transverse noise field if the area of the SQUID loop lies in the symmetry plane dividing the tube in half. Transverse noise fields are also rejected if the area of the SQUID pickup loop lies inside a flat superconducting ring. By taking advantage of symmetry and nodal points, it should then be possible to eliminate pickup from both axial and transverse noise fields.

ACKNOWLEDGMENTS

This research was supported by the state of Texas through the Texas Center for Superconductivity, the Robert A. Welch Foundation and by the Texas Higher Education Coordinating Board Advanced Research Program and Advanced Technology Program.

[1] A. Sezginer and W. C. Chew, IEEE Trans. Magn. **26**, 1137 (1990).
[2] D. B. van Hulsteyn, W. C. Overton, Jr., and E. R. Flynn, Physica B **165&166**, 89 (1990).
[3] D. B. van Hulsteyn *et al.*, Rev. Sci. Instrum. **66**, 3777 (1995).
[4] P. M. Morse and H. Feshbach, *Methods of Theoretical Physics V.II* (McGraw–Hill, New York, 1953), p. 1293.
[5] J. R. Claycomb, Ph.D. thesis, University of Houston, 1998.
[6] B. Cabrera, Ph.D. thesis, Stanford University, 1975.
[7] N. Tralshawala, D. R. Jackson, and J. H. Miller, Jr., IEEE Trans. Appl. Supercond. **5**, 2354 (1995).